Lithos 140-141 (2012) 1–10

Contents lists available at SciVerse ScienceDirect

Lithos

journal homepage: www.elsevier.com/locate/lithos

Timing and conditions of formation of granitoid clasts erupted in recent pyroclastic deposits from Tarawera Volcano (New Zealand)

Phil Shane [a,*], Sonja Storm [a], Axel K. Schmitt [b], Jan M. Lindsay [a]

[a] School of Environment, University of Auckland, Private Bag 92019, Auckland 1142, New Zealand
[b] Department of Earth & Space Sciences, University of California Los Angeles, 595 Charles Young Drive E, Los Angeles, CA 90095, USA

ARTICLE INFO

Article history:
Received 19 July 2011
Accepted 13 January 2012
Available online 26 January 2012

Keywords:
Zircon
U–Th disequilibrium dating
Pluton
Rhyolite
Magma

ABSTRACT

Granitoid clasts in pyroclastic deposits of the 0.7 ka (Kaharoa) eruption from the intra-caldera Tarawera volcano of the Okataina Volcanic Centre (OVC), New Zealand, provide an insight to the plutonic processes beneath one of the most productive Quaternary rhyolite centers on Earth. SIMS U–Th data for 79 granitoid zircon crystals from six clasts reveal a unimodal age spectrum yielding a weighted average model age of 208 ± 4 ka (MSWD = 1.2; n = 72). The remaining crystals are at secular equilibrium and U–Pb analyses indicate that a few of these outliers date back to ~750 ka, a period significantly longer than the known volcanic record at OVC (probably ~550 ka). In contrast, zircon crystallization in co-erupted pumice and lava of the 0.7 ka Kaharoa event, and that of the three preceding rhyolite eruptions, occurred mostly during 0–50 ka, reflecting a separate magmatic history. Brittle deformation features, incipient alteration, and low-$\delta^{18}O$ whole-rock compositions (+3‰) are consistent with a shallow solid intrusion that has interacted with meteoric hydrothermal fluids. However, $\delta^{18}O$ SIMS analyses of zircons (+5.4 ± 0.2‰; n = 11) are consistent with magmatic compositions, and thus meteoric interaction occurred post-emplacement. The Kaharoa granitoids contrast with those ejected in the ~40–60 ka caldera-forming Rotoiti event that were partly molten and display zircon age spectra indistinguishable from those for co-erupted pumices, suggesting the latter were derived from contemporaneous crystal mush. The 0.7 ka Kaharoa case shows that zones of the magmatic system remained solid despite frequent and voluminous magma production that included caldera-forming events. Such long-lived sub-solidus zones in magma systems would act as barriers to melt connectivity and interaction with country rock, but are also a potential source for antecrysts/xenocrysts in subsequent eruptions. This exemplifies how plutonic and volcanic evolution can diverge even in close proximity.

1. Introduction

The frequency and magnitude of Quaternary silicic magmatism is assessed from products of effusive and explosive eruptions at volcanoes. However, volcanic products are likely to be extracts from a more voluminous subterranean source magma or crystal mush zone comprising a rigid framework of interlocking crystals (>50–60%) with interstitial (residual) melt (e.g., Bachmann and Bergantz, 2004; Hildreth, 2004). This concept is consistent with some geophysical interpretations that suggest that voluminous melt-poor bodies exist today within the continental crust at depths as shallow as 5 km (e.g. Table 2 of Bachmann et al., 2007a). Moreover, non-erupted magma volumes are significant and although difficult to quantify, some estimates suggest a ratio of erupted to non-erupted magma of ~1:5 (White et al., 2006). In Quaternary systems that have not undergone extensive uplift and erosion that would expose their intrusive roots, co-magmatic (and xenolithic) plutonic clasts entrained in eruptive deposits are an important source of information on the subterranean magmatism. When such granitoids and their co-erupted pumices contain zircon amenable to U–Th disequilibrium or U–Pb dating (see review by Schmitt, 2011), they provide an opportunity to acquire a more comprehensive insight to the assembly of magmatic systems, and the temporal relationship between plutonism and volcanism.

The Taupo Volcanic Zone (TVZ) of New Zealand (Fig. 1) is one of the most productive Quaternary rhyolite centers on Earth, having produced >10,000 km^3 of silicic magma in the last ~1.6 Ma (e.g., Wilson et al., 2009). Geophysical data have been interpreted as indicating large plume-like structures of interconnected melt beneath the axis of the zone (Heise et al., 2010), and large magma bodies are required for the high thermal energy output at the surface (e.g., Bibby et al., 1995). Thus, the region is the site of on-going large-scale subterranean magmatism. However, due to its youth, plutonic zones have not been exposed by erosion. Other than a few occurrences of intrusive rocks in some of the deeper drill holes (e.g., Browne et al., 1992), rare granitoid clasts within pyroclastic deposits are one of few direct lines of evidence for intrusive processes at TVZ.

* Corresponding author. Tel.: +64 9 3737599.
E-mail address: pa.shane@auckland.ac.nz (P. Shane).

0024-4937/$ – see front matter © 2012 Elsevier B.V. All rights reserved.
doi:10.1016/j.lithos.2012.01.012

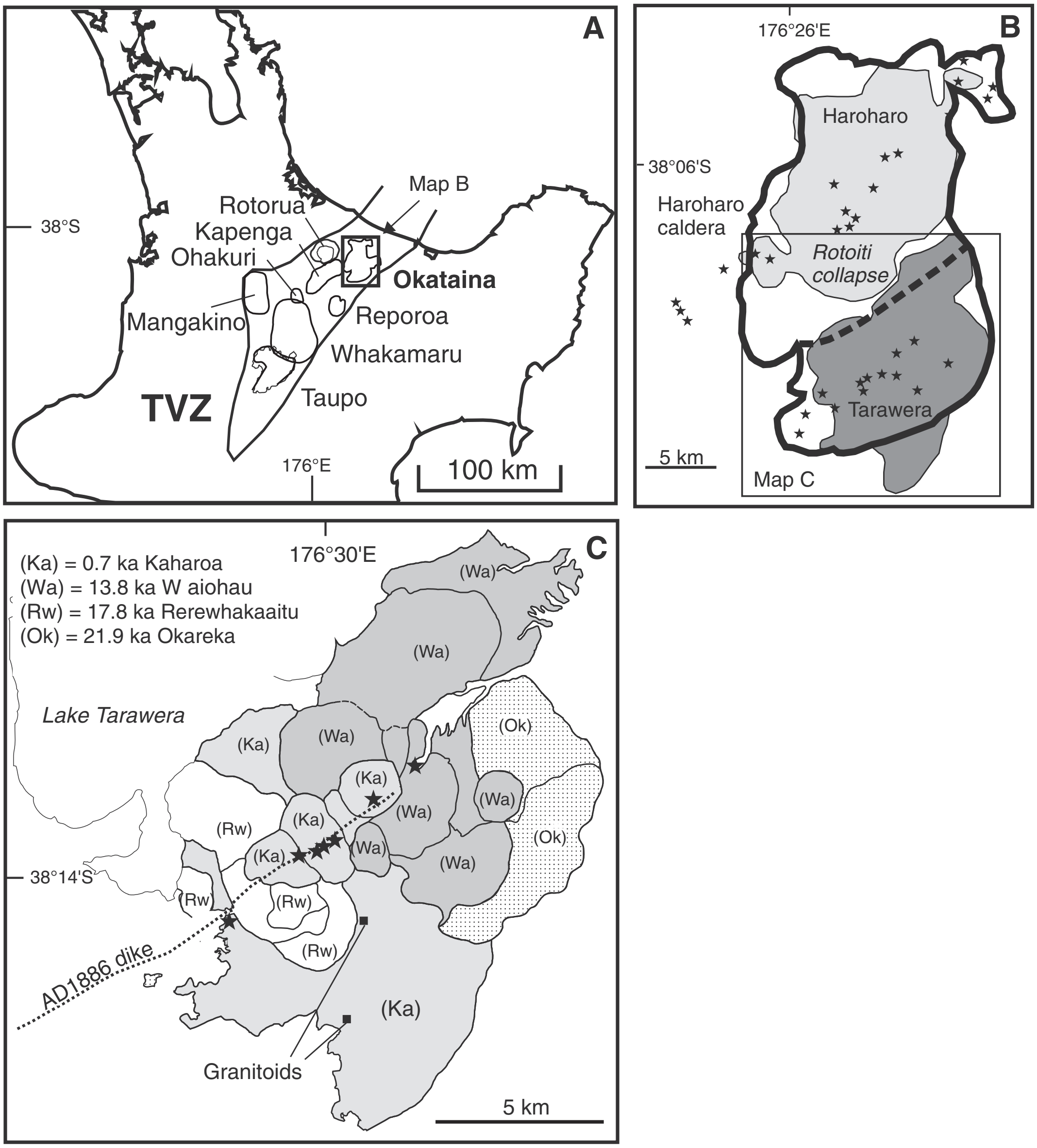

Fig.1. (A) Map of North Island, New Zealand showing the location of the Taupo Volcanic Zone (TVZ) and major rhyolite calderas including Okataina (OVC). (B) Map of OVC showing the Haroharo caldera; the extent of collapse associated with the Rotoiti event; post-22 ka lava and pyroclastic deposits (shaded) and vents (stars). (C) Geologic sketch map of Tarawera Volcano (re-drawn from Nairn 2002) showing the deposits of the four rhyolite eruptions. Stars mark vent locations for the 0.7 ka eruption.

Although such clasts were first documented more than 40 years ago (Ewart and Cole, 1967), little is known about their crystallization history. Charlier et al. (2003) demonstrated contemporaneous crystallization in granitoid and pumice clasts from a ~40–60 ka caldera-forming rhyolite eruption at Okataina Volcanic Centre (OVC) (Fig. 1). Granitoid clasts are rare in post-caldera eruption deposits at OVC. However, the most recent rhyolite eruption (~0.7 ka Kaharoa event) of the intra-caldera Tarawera Volcano (Fig. 1), ejected plutonic blocks (Brown et al., 1998; Nairn et al., 2004).

Here, we present new U–Th and U–Pb SIMS age data on crystal faces and interiors from zircons in granitoid clasts erupted at 0.7 ka to establish the timing of the termination of their crystallization, and compare it to similar data obtained on co-erupted pumice and lava. Along with new whole-rock geochemistry and $\delta^{18}O$ isotope analyses on zircon crystals, we show that the granitoid clasts were derived from a shallow sector of the magmatic system that has remained mostly solid for ~200 ka, surviving assimilation and/or obliteration in numerous eruptions including caldera-forming events. Such sub-solidus sectors point to heterogeneity in crystal mush systems, and are consistent with concepts of periodic 'freeze' and 'thaw', and liberation of antecrysts/xenocrysts in later magmatic events.

2. Tarawera Volcano and Kaharoa eruption

The OVC has been active for at least ~550 ka (Cole et al., 2010; Nairn, 2002). Major caldera-forming ignimbrite eruptions (>100 km^3) occurred at ~325 ka and ~50 ka. The latter event that produced the Rotoiti ignimbrite has been variously dated at ~40–60 ka (Shane and Sandiford, 2003; Wilson et al., 2007). Following this event, volcanism manifested itself as a series of sub-plinian and plinian fall eruptions accompanied by pyroclastic flows (Jurado-Chichay and Walker, 2000). Post-25 ka intra-caldera volcanism has occurred at two sub-parallel loci: Tarawera Volcano and the contemporaneous Haroharo Volcano (Nairn, 2002). Tarawera Volcano (Fig. 1) has been the site of four rhyolite episodes occurring at 21.9 ka, 17.7 ka, 13.7 ka and 0.7 ka (Kaharoa), with a total magma volume of 30 km^3. Each rhyolite episode involved multiple vents along a SW–NE trend, and produced pyroclastic falls and flows, and lava domes (Nairn, 2002). The only historical eruption is a basaltic plinian fissure eruption in AD1886. However, each of the four major rhyolite eruption episodes displays evidence for basaltic interaction (see Shane et al., 2008a). The most recent rhyolite episode, the Kaharoa event, is dated at 636 ± 12 years before AD1950 (~0.7 ka) (Lowe et al., 2008). It involved ~4 km^3 of magma that was primed by repeated injections of basalt magma into a layered body of high-silica rhyolite (Nairn et al., 2004). The eruption occurred from 7 vents along an 8-km linear zone. Early plinian pyroclastic fall and density current deposits were dispersed mostly to the SE, while later deposits display an N and NW dispersal (Nairn et al., 2001). Extrusion of three lava domes and production of block-and-ash flow deposits mark the end of the episode, which lasted an estimated ~5–10 years (Nairn et al., 2001). Rare basaltic enclaves in clasts are found throughout the sequence pointing to mafic intrusion triggering.

The six granitoid clasts examined here were loose rock fragments found in pyroclastic deposits. Sample C3a was collected from unit A, the earliest fall deposit in the sequence, at New Zealand Metric Map grid reference V16/179223. The remaining clasts were collected from unit N (grid reference V16/175197), a late-stage block and ash flow from a dome collapse. Thus, the clasts represent material excavated near the beginning and end of the eruption episode.

3. Analytical techniques

3.1. Geochemistry

Whole-rock major elements of clasts were determined by XRF at the University of Auckland, using a Siemens SRS 3000 sequential X-ray spectrometer with a Rh tube, by Norrish fusion methods (Harvey et al., 1973) (Fig. 2; Supplementary data). Accuracy was checked with the use of 35 international standards. Limits of determination are significantly lower than that measured for all elements (<0.02 wt.%). Trace element data were collected by laser ablation inductively coupled plasma mass spectrometry on fused glass beads at the Australian National University. Instrumentation includes a Lambda Physik Complex 110 ArF (193 nm) Excimer laser and a VG Fusions Plasmaquad PQ2 STE ICPMA spectrometer (see Supplementary data). Instrument calibration was via NIST 612 glass. BCR-2 glass standard was used as an independent assessment of accuracy and precision. Sample analyses were normalized to SiO_2 from XRF data obtained on the same samples. Detection limits were ~5 ppb. Analytical errors of <4% determined from replicate analyses were obtained for all elements reported (see Supplementary data).

3.2. Zircon chronology

Sample preparation included concentration by heavy liquid separation and magnetic separation. A final selection of zircon crystals was made by hand-picking. Cathodoluminescence images were obtained to examine any zoning patterns in sectioned crystals. U–Th isotope analyses on individual zircons were obtained in two sessions using the University of California Los Angeles CAMECA ims 1270 secondary ion mass spectrometer (SIMS) (see Supplementary data). A single-detector collection technique described by Schmitt et al. (2006) was used in session 1, and a multi-collection technique described by Storm et al. (2011) was used in session 2. U/Th relative sensitivities were calibrated from analyses of equilibrium zircon standard AS3 ($^{232}Th/^{238}U = ^{208}Pb/^{206}Pb \times 3.327$; Paces and Miller, 1993) for session 1, and of zircon standard 91500 ($^{232}Th/^{238}U = 0.3559$; Wiedenbeck et al., 1995) for session 2. Accuracy of the relative sensitivity calibration and background corrections were verified by replicate analysis of AS3 interspersed with the unknowns. The following (^{230}Th)/(^{238}U) values were obtained for the first session: 1.016 ± 0.007 (MSWD = 0.88; n = 23) and for the second session: 1.001 ± 0.014 (MSWD = 0.10; n = 10).

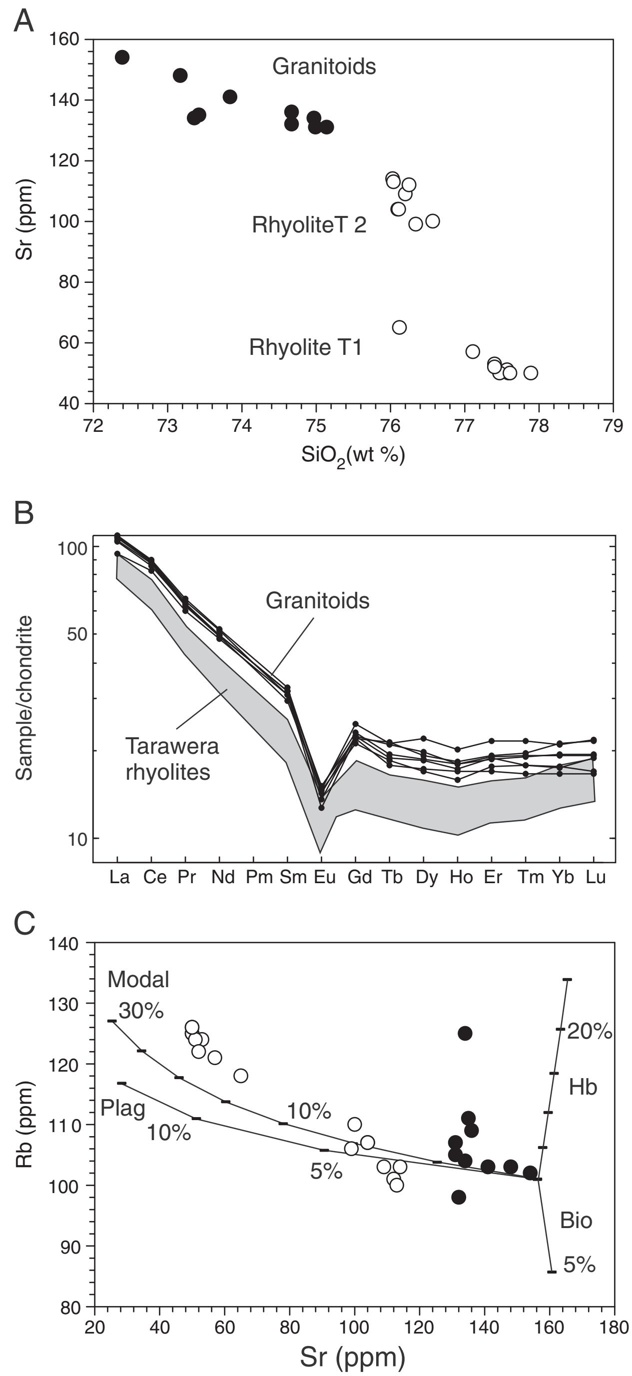

Fig. 2. (A) Whole rock composition of Kaharoa granitoids (this study) compared to that of co-erupted rhyolites (Nairn et al., 2004). (B) REE composition of Kaharoa granitoids (this study) compared to that of Tarawera rhyolites (Shane et al., 2008a,b). Chondrite normalization values are those of Sun and McDonough (1989). (C) Fractional crystallization trends (curves) model parental melt that is represented by the least evolved granitoid composition (see text). Partition coefficients used: plagioclase $D_{Rb} = 0.105$; $D_{Sr} = 11.73$ calculated from Blundy and Wood (1991) using assuming An_{25} and T = 730 °C; hornblende $D_{Rb} = 0.02$, $D_{Sr} = 0.77$ (Ewart and Griffin, 1994); biotite $D_{Rb} = 4.2$, $D_{Sr} = 0.447$ (Mahood and Hildreth, 1983), and quartz D = 0. Model mineralogy based on average pumice 45% plagioclase, 45% quartz, 10% biotite, and trace orthopyroxene and hornblende (Nairn et al., 2004).

The zircons analyzed are 100–250 μm in length. They were immersed in ~50% HF at room temperature for approximately 3 min to remove any adherent material. The crystals were then embedded in indium (In) metal and coated with gold. Analyses were carried out on unpolished crystal faces (‘rim’ analyses) with 3–5 μm depth excavation at ~25–30 μm diameter lateral resolution. For sample T022, the same crystals were then polished (ground down ~5 μm) and analyzed as spot analyses ('interior' analyses).

U–Th model ages are calculated as two-point isochrons through the zircon and a whole rock composition, assuming initial ($^{230}Th/^{232}Th$) in the zircon crystal is the same as in other OVC rhyolites (Fig. 3). We used the average of three Rotoiti and Earthquake Flat analyses with ($^{230}Th/^{232}Th$) = 0.736 ± 0.013 and ($^{238}U/^{232}Th$) = 0.732 ± 0.006 (Charlier et al., 2003) to represent the model magma. Although there is no way of determining these values for the melt which crystallized the granitoid zircon, it is reasonable to use the above model composition because it represents a secular equilibrium composition that is typical of the OVC. Minor variations in ($^{230}Th/^{232}Th$) and ($^{238}U/^{232}Th$) in OVC rhyolites are largely insignificant for the uncertainties of our model ages because of the strong leverage of zircon on the model isochron. This can be illustrated by comparison with two-point isochron model ages that use whole rock data for the Kaharoa granitoid with ($^{230}Th/^{232}Th$) = 0.522 ± 0.004 and ($^{238}U/^{232}Th$) = 0.405 ± 0.008 (M. Turner pers. comm. 2011). This produces ages that are only on average 5% younger than those calculated using Rotoiti/Earthquake Flat compositions. For each crystal, this age difference is less than analytical uncertainty. However, we prefer the model ages based on Rotoiti/Earthquake Flat compositions because the granitoid samples display signs of incipient alteration by hydrothermal fluids (see Section 4). Regardless, the model age difference resulting from the selection of a melt composition does not significantly impact our conclusions.

Age spectra and peaks based on a population of crystals were determined from probability density function (PDF) curves generated in Isoplot (Ludwig, 2003). All ages are quoted with 1 σ error unless otherwise stated.

Crystals that were in secular equilibrium (within 1 sigma uncertainty) were also analyzed for U–Pb (see Supplementary data) applying corrections for common-Pb based on measured ^{207}Pb as well as for ^{230}Th disequilibrium outlined in Schmitt et al. (2003).

3.3. Zircon δ^{18}O isotopes

Zircon geochronological analysis pits with implanted ^{16}O (from the mass-filtered O^- primary beam used for U–Th–Pb analysis) were removed via grinding and polishing (~5 μm) prior to SIMS oxygen isotope analysis (see Supplementary data). This resulted in culling of smaller crystals and only the remaining larger crystals could be analyzed for $\delta^{18}O$ using the ims 1270 ion microprobe following established

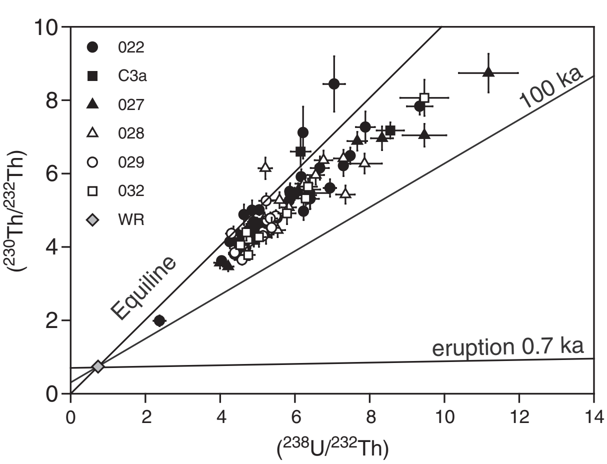

Fig. 3. Zircon U–Th model-age data for the Kaharoa granitoid zircon crystal faces (sample 022 represents crystal faces and interiors). The equiline and isochrons for the eruption age and 100 ka are shown for reference. Error bars represent 1σ analytical uncertainties.

procedures (Trail et al., 2007). Standard zircon AS3 ($\delta^{18}O$ value of + 5.34‰; Trail et al., 2007) placed on the same mount together with the unknowns was used to correct for instrumental mass fractionation ($\alpha = 0.9997$). The reproducibility of the bracketing AS3 analysis was 0.4‰ (1 σ error; n = 8) which we adopt as an estimate for the external reproducibility of individual analyses.

4. Petrography and geochemistry

Plutonic clasts in Kaharoa eruption deposits have been described as medium-grained biotite granodiorites (Brown et al., 1998; Ewart and Cole, 1967), or more generally as granitoids (Nairn et al., 2004). Mineralogically, they comprise ~35% quartz, 40% plagioclase, 20% alkali feldspar and ~3–5% biotite, with trace (<0.1%) accessory phases including Fe–Ti oxides, hornblende, apatite and zircon. The granitoids have an equigranular texture with small interstitial patches of finer crystals. Quartz is commonly subhedral to anhedral, and in places occurs as granophyric intergrowths with alkali feldspar. Large quartz crystals display zoning patterns and resorption horizons in CL imaging (Shane et al., 2008a). Alkali feldspars have Na-rich patches resulting from exsolution, and a few crystals display a 'cloudy' appearance, resulting from micro-inclusions, indicative of alteration. Euhedral to subhedral plagioclase crystals display zoning and resorbed cores. Biotite occurs as euhedral and subhedral laths with edges displaying incipient alteration. It contains common micro-inclusions of Fe–Ti oxides, zircon and apatite. Dislocation features and 'wavy' extinction indicative of strain deformation are present in plagioclase and quartz, and Shane et al. (2008a) reported annealed laminae in quartz visible in CL imaging indicative of brittle deformation.

Despite optical evidence for incipient alteration in the granitoid clasts, smooth chondrite-normalized REE patterns that are sub-parallel to those of the Tarawera rhyolite, and the lack of elemental anomalies (e.g., La or Ce), reflect immobility (e.g., Kerrich and Wyman, 1996), and indicate alteration is not pervasive (Fig. 2). Whole rock analyses indicate that the clasts are granitoids that display a narrow compositional range (SiO_2 = 72–75 wt.%), and are distinguished from co-erupted pumice and lava that display higher SiO_2 contents (~76–78 wt.%) (Fig. 2A). The Kaharoa rhyolites comprise two homogeneous magma types (T1 and T2) that were sequentially erupted (Nairn et al., 2004), and are distinguished by various trace element concentrations (e.g. Sr, Fig. 2A). Early fall deposits comprise T1 type magma; and late-stage falls and domes comprise T2 type magma. Minor intermediate deposits comprise a mixture of T1 and T2 lapilli (Nairn et al., 2004). The granitoid clasts also have relatively narrow compositional ranges in trace elements (e.g., Zr = 135–166 ppm; Sr = 134–154 ppm; $\sum$REE = 125–138 ppm), which are slightly enriched relative to that of co-erupted pumice compositions (Zr = 85–140 ppm; Sr = 50–115 ppm; $\sum$REE = 101–111 ppm). Both granitoid and pumice/lava clasts display negative Eu anomalies (Eu/Eu* = 0.46–0.58 and 0.43–0.66, respectively) and high LREE/HREE ratios (La/Yb_N = 3.8–5.5 and 4.2–5.0, respectively) (Shane et al., 2008a) (Fig. 2B). Plagioclase-dominated fractionation can explain variations in Rb and Sr abundances within the rhyolites relative to model melts represented by granitoid compositions (Fig. 2C). However, enriched REE concentrations in the granitoids are the opposite of what would be predicted for a granitoid parent, unless accessory minerals had accumulated. Also, U–Th zircon ages for the rhyolites and granitoids demonstrate the absence of direct consanguinity (see Section 6.1). The granitoid compositions (M = (K + Na + 2 Ca)/(Al*Si) = 1.40–1.46) have zircon saturation temperatures of 771–789 °C based on the algorithm of Watson and Harrison (1983). Fe–Ti oxide equilibrium suggests temperatures of 730–750 °C (Brown et al., 1998). Thus, it is likely that zircon crystallized in the magma rather than representing a relict component.

5. Zircon crystallization ages and δ^{18}O isotope compositions

U–Th spot ages were determined on the crystal faces of 79 zircons from the six granitoid clasts (Fig. 3; Supplementary data). The number of crystals analyzed per sample was largely controlled by the limited amount of material per plutonic clast, and the availability of crystals sufficiently large for mounting (Fig. 4). The weighted average of the entire crystal face population is 216 ± 6 ka, but with a MSWD = 1.83 which is significantly elevated relative to the permissible range for n = 79 (Mahon, 1996). Seven analyses yielded near-secular equilibrium (~350 ka) model ages which were replicated in crystal interior analyses or U–Pb ages that were within 1σ uncertainty of secular equilibrium (see below). Excluding these analyses, we obtained a unimodally-distributed population with a weighted average age of 208 ± 4 ka and an acceptable MSWD = 1.18 (n = 72) (Fig. 5). This model age is indistinguishable with the zircon isochron age of the crystal rim population (excluding secular equilibrium crystals) of 195 + 19/− 16 ka (MSWD = 1.16; n = 72).

Spot analyses were obtained on polished interiors of 14 of the zircons in sample T022 (Fig. 4). Of these analyses, 3 plot above the equiline (overlapping it within 2 σ error), and 9 overlap within error (1 σ) of their accompanying crystal face age. Only one crystal (grain 13) has a resolvable (within 2 σ) difference between rim and interior age of ~170 ka. The 11 crystal interior ages (excluding three analyses with $^{230}Th/^{238}U$ activity > 1) yield a weighted average age of 234 ± 4 ka (MSWD = 1.4).

U–Pb ages for 6 crystal rims have generally low radiogenic ^{206}Pb yields, and are within uncertainty of zero age, implying that they are close to the secular equilibrium of ~350 ka indicated by U–Th analyses. Of the secular equilibrium crystal rims, only two meaningful $^{206}Pb/^{238}U$ ages were determined: 412 ± 138 ka and 765 ± 78 ka, and only the second age is resolvedly older than near-secular equilibrium age of ~350 ka.

$\delta^{18}O_{SMOW}$ in zircon was determined on 11 crystal interiors which yielded an average value of 5.4 ± 0.2‰ (standard error of average; MSWD = 3.4). For comparison with whole-rock values, we account for oxygen isotope fractionation between melt and zircon using the experimental calibration of $^{18}O/^{16}O$ fractionation between quartz and zircon as a proxy (Trail et al., 2009). This amounts to addition of approximately + 2‰ (at ~800 °C zircon saturation temperature) to the measured zircon $\delta^{18}O$ value (= ~7.4‰). The slightly elevated MSWD could indicate heterogeneity in the granitoid zircon population (with an overall range between 4.3 and 6.5‰ at an external reproducibility of 0.4‰). However, the significance of this diversity is marginal because we cannot completely rule out minor bias that could result from beam overlap onto crystal imperfections such as cracks or inclusions. Regardless, even the lowest magmatic value calculated from zircon significantly exceeds the value for the whole-rock (+ 3.03‰) at the 8 σ level.

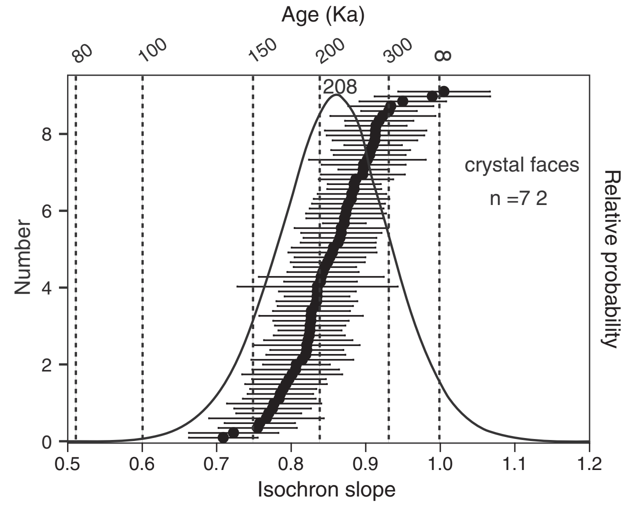

Fig. 5. Probability density function curve, and rank order plot (ROP) showing distributions of U–Th model ages of zircon crystal faces from all Kaharoa granitoid samples combined, but excluding those in secular equilibrium. Model ages are based on isochron slopes to incorporate symmetrical errors. For the ROP, 1σ error bars are shown for each data point.

6. Discussion

6.1. Age relationship between Tarawera rhyolites and granitoid clasts

The small size of the granitoid clasts (<10 cm) and their occurrence in pyroclastic deposits prevents a definitive assessment of whether they represent more than one intrusive body. However, the similarity in zircon age spectra of all clasts (Figs. 4 and 5) is consistent with a single emplacement unit.

Textural, mineralogical and geochemical features of Tarawera rhyolites are consistent with their rapid generation (<1 ka) via mafic intrusion into a long-lived (>20 ka) silicic crystal mush zone (see Shane et al.,

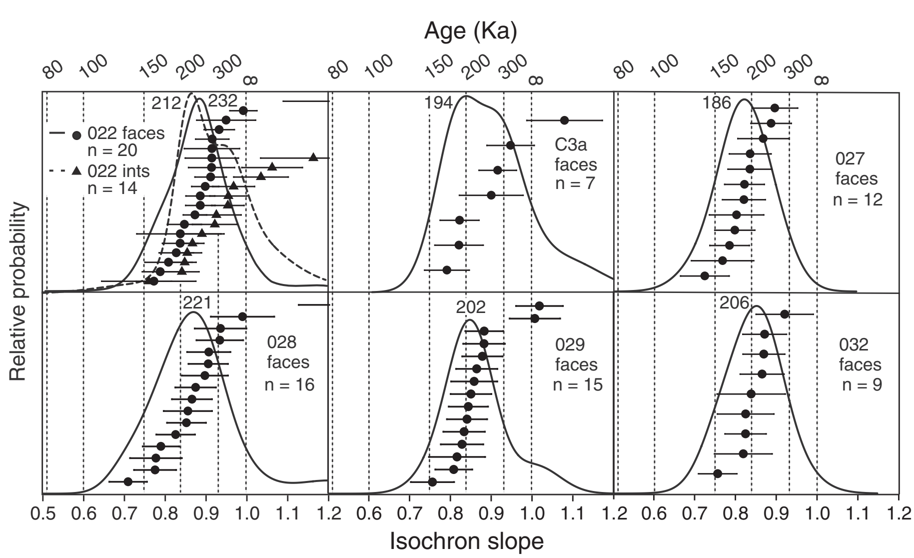

Fig. 4. Probability density function curve and rank order plot (ROP) showing distributions of U–Th model ages of zircon crystal face analyses from Kaharoa granitoid samples. Crystal interior analyses are also shown for sample 022. Model ages are based on isochron slopes to incorporate symmetrical errors. For the ROP, 1σ error bars are shown for each data point. The full data set is shown, including those in secular equilibrium.

2008a). The granitoid clasts have a broadly similar mineralogy and geochemistry to the rhyolites. If the granitoid clasts represented the crystal mush from which melt extraction (= rhyolites) occurred, fractional crystallization of a plagioclase-dominated mineralogy could explain the depletion and enrichment of compatible and incompatible elements, respectively, in the rhyolites relative to the granitoids (Fig. 2C). However, disparate zircon crystallization histories (described below) demonstrate the granitoids clasts were not a contemporaneous partly-molten body during rhyolite magma production.

The zircon assemblage in granitoid clasts is significantly older than that in the accompanying rhyolites (Fig. 6). Klemetti et al. (2011) obtained SIMS U–Th age data on 90 zircon crystals from the Kaharoa rhyolite by analyzing cores and interiors of sectioned crystals. The ages are in the range of ~2 to >200 ka, with nearly all crystals <50 ka (Fig. 6A). Storm et al. (in press) obtained data on a further 64 crystals via analyses of un-polished crystal faces and continuous profiling into the crystals. They obtained ages within error of the eruption age (0.7 ka), dating back to ~79 ka (oldest crystal interiors). The generally younger ages presented by Storm et al. (in press) reflect the shallower profiling compared to the deep crystal sectioning by Klemetti et al. (2011). Excluding crystals in secular equilibrium, two of the oldest crystal cores with determinable ages (173 + 62/−37 ka; 188 + 63/−37 ka) (Klemetti et al., 2011) do overlap in time with the granitoid zircon population (~200 ka). This could be interpreted as a common parental magma system in space and time. Alternatively, the oldest zircon crystals in the rhyolites could be xenocrysts, and the granitoid clasts could represent an unrelated intrusive episode in the system. Regardless, the granitoid clasts lack the young zircon population that dominates the rhyolite zircon age spectra, demonstrating the former was in a sub-solidus state for much of the recent history of the volcano. Zircon age data from other post-22 ka Tarawera eruption deposits also show that most of the crystallization occurred post-50 ka (Storm et al., 2011, in press) (Fig. 6B).

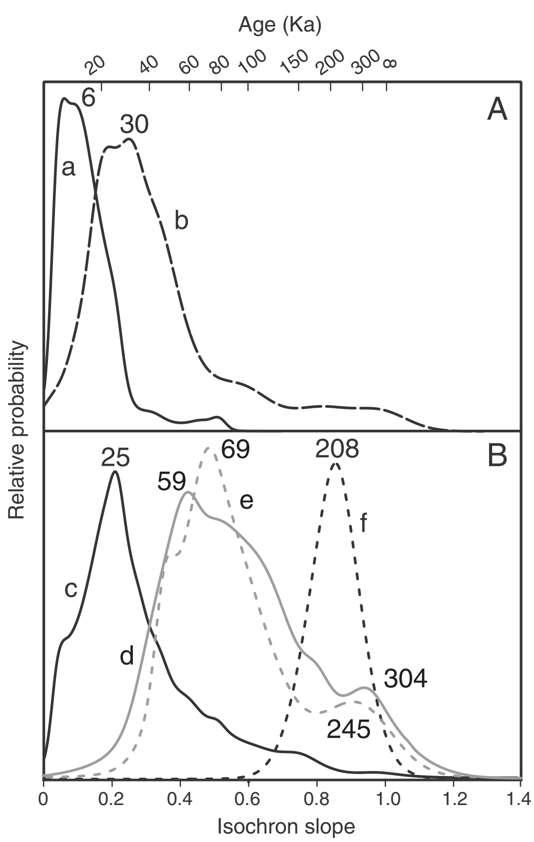

Fig. 6. Summary of zircon age data plotted as probability density function curves. (A) Curve (a) Kaharoa rhyolite zircon from crystal face and interior analyses (n = 123) (Storm et al., 2011), and curve (b) interior analyses from sectioning of crystals (n = 66) (Klemetti et al., 2011). (B) Curve (c) Tarawera post-22 ka rhyolite zircons from crystal face and interior analyses (n = 487; Klemetti et al., 2011; Storm et al., in press); curve (d) Rotoiti rhyolite zircon interior analyses (n = 72); curve (e) Rotoiti granitoid zircon interior analyses (n = 22) (Charlier and Wilson, 2010; Charlier et al., 2003); and curve (f) Kaharoa granitoids crystal face and interior analyses (n = 83; this study). Data exclude analyses at secular equilibrium. Numbers at peaks represent ages (ka).

Zircons in rhyolite samples show evidence of liberation from sub-solidus storage, but post-dating the zircon history of the granitoid clasts. In the Kaharoa rhyolite, some crystal faces that lack resorption features, are up to ~24 ka in age suggesting that crystallization ceased long before eruption (0.7 ka). Age–depth profiling of the zircons in all of the Tarawera rhyolites reveals protracted continuous and discontinuous crystal growth over periods up to ~100 ka (Storm et al., 2011, in press). However, the data and CL imaging provide no evidence for old, highly corroded crystal cores that could represent a separate phase of crystallization such as that recorded in the granitoid clasts. Thus, more recent episodes of magma formation have either stripped the magmatic system of most of its older zircon population in thermal events associated with reactivation, or new zircon crystallization volumetrically swamped the older population. Alternatively, the areas of more recent magma production and that of granitoid clast source(s) were spatially separate (see Section 6.2). Regardless, the granitoid clasts represent part of the system immediately beneath the volcano that escaped interaction in magma production for some time.

6.2. Residence zone of the source(s) of granitoid clasts

Several features point to shallow, sub-solidus conditions for the granitoid clasts prior to entrainment and eruption:

(1) The clasts display a distinctly lower whole-rock $\delta^{18}O_{SMOW}$ isotope value (+3.03‰) compared to more typical magmatic values of >7.5‰ for rhyolites from OVC (Brown et al., 1998; Nairn et al., 2004). Low-$\delta^{18}O$ granitoid clasts have been reported elsewhere (Bacon et al., 1989; Schmitt and Vazquez, 2006), and have been attributed to interaction between shallow sub-solidus intrusion and deep penetrating low-$\delta^{18}O$ meteoric-sourced, hydrothermal fluids.
(2) Incipient alteration of feldspar and biotite in the granitoid clasts is consistent with interaction with hydrothermal fluids, and is not evident in OVC rhyolite pumice and lava.
(3) Brittle strain deformation features are ubiquitous in feldspar and quartz in the granitoid clasts. Such features are conspicuously absent in phenocrysts from OVC rhyolite pumice and lava clasts.
(4) Compositional separation in feldspars indicates exsolution. Retrograde cation exchange is indicated by low, two-feldspar temperature estimates of ~645 °C (Brown et al., 1998).

$\delta^{18}O$ values for the granitoid melt (~7.4‰) determined here from zircon oxygen isotope analyses are typical of magmatic compositions in the TVZ (e.g., Brown et al., 1998) and provide no evidence for crystallization from a low-$\delta^{18}O$ melt. Zircon is inert even to extensive propylitic to potassic hydrothermal alteration (Schmitt and Hulen, 2008) and reliably preserves magmatic $\delta^{18}O$ values. The depletion in whole-rock $\delta^{18}O$ is therefore the result of interaction with hydrothermal fluids which occurred after emplacement. We note that alteration was not pervasive because whole-rock REE and trace element patterns are consistent with immobility (see Section 4).

In summary, several lines of evidence indicate the granitoid clasts are from a high-level, sub-solidus 'carapace' of the larger magma system, or a separate high-level intrusion, that was accidently sampled in the Kaharoa eruption event.

Magnetotelluric and gravity data from OVC are consistent with conductive and porous rock down to ~3 km, interpreted to be volcaniclastics and/or pyroclastics overlying high resistivity rock (Seebeck et al., 2010). Mineralogical, geochemical and volatile constraints place crystallization of major mineral phases in Tarawera rhyolites at ~7–8 km (Shane et al., 2008a). Current seismicity places the brittle-to-ductile transition at depths of 6–7 km (Bryan et al., 1999). Thus, the most likely zone for brittle crystalline granitoids is the 3–7 km zone. Plutonic rocks have been rarely encountered in deep drill cores in the upper ~3 km of the TVZ crust. Diorite has been encountered in one core, at a depth of ~2.2 km, some 60 km SW of the OVC (Browne et al., 1992). This occurrence demonstrates that small high-level intrusions are present. However, the large magma bodies (exceeding erupted volumes) required for the high thermal energy output of the TVZ at present (e.g., Bibby et al., 1995) must reside at greater depths.

6.3. Comparison with Rotoiti granitoid clasts and older phases of OVC volcanism

The only other granitoid material studied in detail from OVC is clasts ejected in the ~40–60 ka caldera-forming Rotoiti event. They are broadly similar to Kaharoa granitoid clasts in whole rock chemistry, mineralogy, and Sr and Nd isotope composition (Brown et al., 1998). However, several characteristics distinguish Rotoiti granitoid clasts from those in Kaharoa deposits:

(1) They contain abundant interstitial glass (up to 30% modal), considered by Burt et al. (1998) to be residual melt due to sharp contacts between euhedral crystals and glass.
(2) They display pronounced granophyric intergrowth (Burt et al., 1998), similar to textures described in the literature as involving several episodes of volatile pressure release (e.g., Lowenstern et al., 1997).
(3) Brittle deformation features are absent, but slump folding indicating ductile deformation is recorded in one clast (Burt et al., 1998).
(4) Whole rock $\delta^{18}O$ values (+7.4–7.9‰) are magmatic and comparable to co-erupted Rotoiti rhyolites and other OVC rhyolites (Brown et al., 1998).
(5) The U–Th zircon age spectrum from the Rotoiti granitoid clasts is comparable to that of the co-erupted rhyolite pumice (Fig. 6) indicating contemporaneous residence and crystallization (Charlier et al., 2003).

Thus, the Rotoiti granitoid was a contemporaneous and partly molten magma body that was disrupted by the evacuation of the main Rotoiti (rhyolite) magma body during caldera formation (see Charlier et al., 2003) (Fig. 7). This contrasts with the crystallization history of the Kaharoa granitoid that indicates little or no interaction with magma-forming processes post-200 ka. Some overlap in the age spectra of Tarawera rhyolites and Rotoiti rhyolites and granitoid (Fig. 6B) points to contemporaneous crystallization across the OVC magmatic system, and thus a potentially extensive crystal mush zone (Fig. 7). However, diverging petrologic and crystallization trends in eruption deposits demonstrate that melts were not necessarily connected (e.g., Shane et al., 2008a; Storm et al., 2011, in press).

The Rotoiti and Kaharoa granitoid clasts display similar Sr and Nd isotope ratios to volcanic rocks erupted from the TVZ (Brown et al., 1998), providing no evidence for significant differences in source rocks. Both granitoid groups also display enriched LREE/HREE ratios and negative Eu anomalies similar to OVC rhyolites (Fig. 2B) indicating they are products of plagioclase, hornblende, and zircon fractionation, and are not cumulate bodies. Thus, the rhyolites and granitoids are both considered to be extracts from a crystal mush zone, and the latter have cooled to a crystalline state prior to eruption. A significant difference between the granitoids and rhyolites of the OVC (and TVZ in general), is the ubiquitous absence or scarcity of K-feldspar in the latter. The high-SiO_2 melts (glasses) of OVC rhyolites plot near the haplogranite eutectic (e.g. Shane et al., 2008b). Thus, K-feldspar in the granitoids can be explained by final crystallization of silicic interstitial melt.

The oldest zircon in the Kaharoa granitoid clasts (~750 ka) indicates that magmatic activity beneath OVC spans nearly half of the known rhyolite history of the TVZ (~1.6 Ma, Wilson et al., 2009). The earliest volcanism at OVC is difficult to determine because poorly-dated, contemporaneous calderas (Rotorua and Kapenga, Fig. 1) border the OVC making medial and distal deposits difficult to source, and early volcanism could have been obliterated by later eruptions. Caldera-forming eruptions occurred at 890 and 240 ka at Kapenga, and at 240 ka at Rotorua (summary by Wilson et al., 2009). The earliest deposits potentially representing caldera formation at OVC are the “quartz–biotite tuffs” or ignimbrites dated at ~550 ka (Cole et al., 2010). The Matahina Ignimbrite eruption dated at 325 ka (Cole et al., 2010) was also a major collapse event (Nairn, 2002). Most of the zircon crystallization (~200 ka) represented in the Kaharoa granitoid clasts corresponds to a period of poor temporal constraint at OVC. This interval, between the 325 ka Matahina and ~40–60 ka Rotoiti ignimbrites, includes volumetrically minor pyroclastic deposits that are mostly pre-240 ka in age (Nairn, 2002), and the voluminous (Tutaeheke) lavas southwest of Tarawera (Cole et al., 2010). The zircons in the granitoid clasts confirm intrusive activity at this time in the vicinity of the future Tarawera Volcano.

Old zircons in eruption deposits suggest that magmatism significantly pre-dates the surface expression of volcanism at some TVZ volcano centers, and spans much of the TVZ's history. Zircons of ~500 ka are found in pumice from Taupo Volcano, where surface activity mostly post-dates 300 ka (Charlier et al., 2005), and zircons of ~600 ka occur in Whakamaru ignimbrite that produced the Whakamaru caldera at ~340 ka (Brown and Fletcher, 1999). A caveat is that the early history of volcanism at these volcanoes could have been largely obliterated. Even older magmatic zircons (~900–1900 ka) have been found in deposits of the Mangakino center (McCormack et al., 2009; Wilson et al., 2008), the earliest locus of volcanism in TVZ. Together with ~750 ka zircon from the OVC (this study), the old zircons suggest prolonged and contemporaneous magmatism throughout much of the central TVZ, and no spatial–temporal patterns. This supports the concept of a ‘central TVZ batholith’, inferred from the overlap of volcanic centers and extensive melt-bearing zones at depth as discussed by Wilson and Charlier (2009).

6.4. Lessons from plutonic clast studies

Plutonic clasts can represent different stages of the magmatic evolution of a volcano: crystallization can coincide with previous episodes of eruption at the volcano (e.g., Bacon and Lowenstern, 2005), or reflect periods that lacked accompanying eruptions, thus representing wholly intrusive phases (e.g., Lowenstern et al., 2000; Vazquez et al., 2007). In other cases, the zircon age spectra for granitoid and co-erupted pumice/lava clasts are indistinguishable, pointing to contemporaneous magma bodies in various states of solidification leading up to eruption (Bachmann et al., 2007b; Charlier et al., 2003). In cases where the plutonic clasts contain interstitial (residual) glass, the clasts represent sampling of a contemporaneous crystal mush, supporting the recent concepts of rhyolites representing melt extraction events from a crystal-rich zone (Bachmann and Bergantz, 2004; Hildreth, 2004).

Co-erupted plutonic and volcanic blocks at Soufriere Volcanic Complex, St Lucia have indistinguishable zircon age populations inherited from previous magmatic events, and provide strong evidence for recycling and cannibalization of plutonic forerunners by subsequent eruption episodes (Schmitt et al., 2010). The age spectra are protracted (>100 ka) and polymodal, revealing progressive reactivation and homogenization of the magmatic system over time. This contrasts with the Tarawera magma system where the granitoid clasts

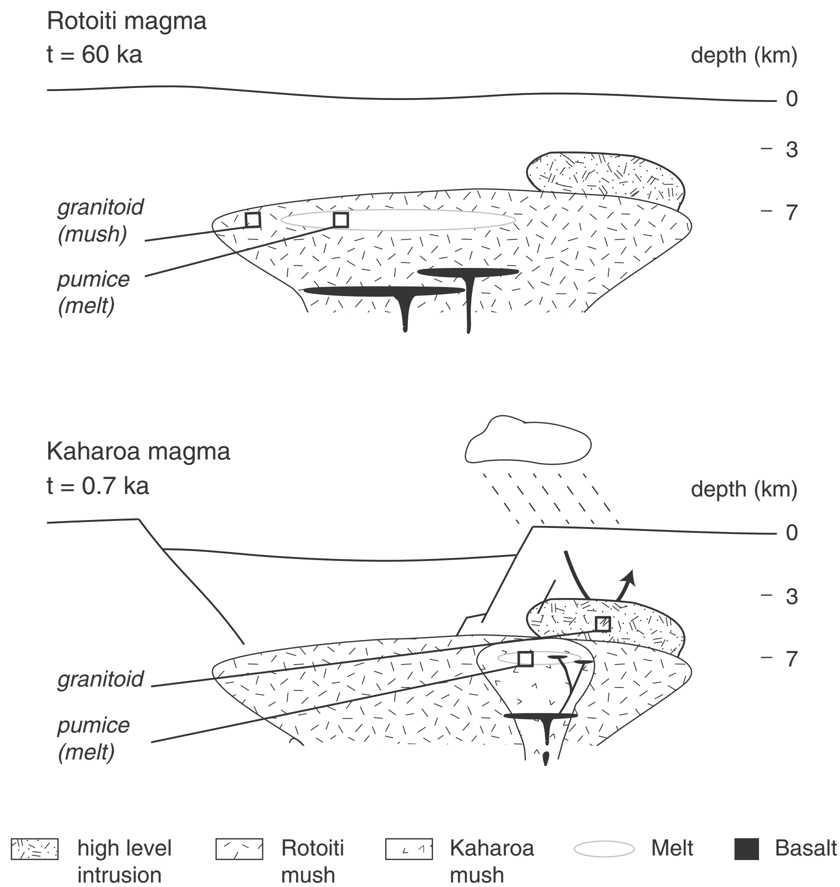

Fig. 7. Conceptual drawing of the relationship between granitoid source areas and co-erupted rhyolites in the ~40–60 ka Rotoiti and 0.7 ka Kaharoa eruptions. In the Rotoiti caldera-forming event, the granitoid material was partly molten and its zircon crystallization was contemporaneous to that recorded in the erupted melt (rhyolite pumice). In the Kaharoa event, the granitoid material was excavated from a high level intrusion that had not been involved in magma production for some time. Its shallow position allowed interaction with meteoric hydrothermal fluids. The lateral extent of the zones is idealized, and may be more heterogeneous.

erupted at 0.7 ka remained mostly solid for ~200 ka, surviving assimilation and/or obliteration in numerous eruptions including caldera-forming events. Such sub-solidus regions of the magma system could act as barriers to interaction with the surrounding wall-rocks and active (melt-bearing) parts of the magmatic system. This is consistent with petrologic evidence for limited connectivity between co-erupted melts that characterize Tarawera's magmatic history (Shane et al., 2008a).

The contrasting crystallization histories of the granitoids in the Rotoiti and Kaharoa deposits, and their relationship to their respective accompanying rhyolite melts, are striking (Fig. 6). The difference could reflect the degree of magma draw-down during eruption. The voluminous Rotoiti event involved caldera collapse reflecting extensive magma drainage and thus tapping of the underlying crystal mush zone (= granitoid). The Kaharoa event was an order of magnitude smaller and not associated with collapse. The granitoids instead were simply opportunistic excavation of wall-rock in the conduit (Fig. 7).

7. Conclusions

1. U–Th zircon ages from Kaharoa granitoid clasts ejected at 0.7 ka reveal a crystallization event at 208 ± 4 ka (MSWD = 1.2), a period poorly constrained from the surface record of volcanism at OVC. A few outlier crystals date back to ~750 ka, which precedes the known volcanic record within the OVC (~550 ka), demonstrating the chronological value of these rare clasts.
2. The post-22 ka intra-caldera rhyolite volcanism represents reactivation of crystal mush via mafic intrusion (Shane et al., 2008a). In contrast to the granitoid clasts, nearly all of the zircon crystallization in these rhyolites occurred at 0–50 ka (Klemetti et al., 2011; Storm et al., in press). The old age of the granitoid zircon population illustrates how parts of a magmatic system can be mostly solid despite frequent and voluminous magma production that included caldera-forming events. Such long-lived sub-solidus zones would act as barriers to melt connectivity and interaction with country rock, but also a potential source of antecrysts/xenocrysts in subsequent eruptions.
3. Textural, geochemical and isotopic features of the Kaharoa granitoid clasts are consistent with shallow intrusion, brittle deformation, and interaction with hydrothermal fluids. However, $\delta^{18}O$ isotope analyses of zircon are typical of magmatic values, indicating shallow interaction with hydrothermal fluids was post-emplacement. Geophysical data and petrologic constraints provided by the rhyolites imply a residence depth of 3–7 km. A laterally extensive, cooling plutonic zone is required to explain the exceptional heat flow that characterizes much of the TVZ at present.
4. The Kaharoa granitoid clasts differ significantly from those erupted in the ~40–60 ka Rotoiti caldera-forming event at OVC. The latter were a partly molten crystal mush that was entrained during eruption of the main crystal-poor rhyolite body, and granitoid–rhyolite zircon crystallization was largely synchronous (e.g., Charlier et al., 2003). This highlights the diversity of plutonic environments that clasts in pyroclastic eruptions can potentially excavate.

Acknowledgments

The ion microprobe facility at UCLA is partly supported by a grant from the Instrumentation and Facilities Program, Division of Earth Sciences, National Science Foundation. We acknowledge the following funding: GNS Science subcontract (PS), New Zealand Earthquake Commission (JL), and University of Auckland Doctoral Scholarship (SS). Ian Smith assisted with the acquisition of trace element data. Charles Bacon, Colin Wilson and an anonymous reviewer provided valuable comments.

Appendix A. Supplementary data

Supplementary data to this article can be found online at doi:10.1016/j.lithos.2012.01.012.

References

Bachmann, O., Bergantz, G.W., 2004. On the origin of crystal-poor rhyolites; extracted from batholithic crystal mushes. Journal of Petrology 45, 1565–1582.
Bachmann, O., Miller, C.F., de Silva, S.L., 2007a. The volcanic–plutonic connection as a stage for understanding crustal magmatism. Journal of Volcanology and Geothermal Research 167, 1–23.
Bachmann, O., Charlier, B.L.A., Lowenstern, J.B., 2007b. Zircon crystallization and recycling in the magma chamber of the rhyolitic Kos Plateau Tuff (Aegean Arc). Geology 35, 73–76.
Bacon, C.R., Lowenstern, J.B., 2005. Late Pleistocene granodiorite source for recycled zircon and phenocrysts in rhyodacite lava at Crater Lake, Oregon. Earth and Planetary Science Letters 233, 277–293.
Bacon, C.R., Adami, L.H., Lanphere, M.A., 1989. Direct evidence for the origin of low-^{18}O silicic magmas: quenched samples of a magma chamber's partially-fused granitoid walls, Crater Lake, Oregon. Earth and Planetary Science Letters 96, 199–208.
Bibby, H.M., Caldwell, T.G., Davey, F.J., Webb, T.H., 1995. Geophysical evidence on the structure of the Taupo Volcanic Zone and its hydrothermal circulation. Journal of Volcanology and Geothermal Research 68, 29–58.
Blundy, J.D., Wood, B.J., 1991. Crystal–chemical controls on the partitioning of Sr and Ba between plagioclase feldspar, silicate melts, and hydrothermal solutions. Geochimica et Cosmochimica Acta 55, 193–209.
Brown, S.J.A., Fletcher, I.R., 1999. SHRIMP U–Pb dating of the pre-eruption growth history of zircons from the 340 ka Whakamaru Ignimbrite, New Zealand; evidence for >250 k.y. magma residence times. Geology 27, 1035–1038.
Brown, S.J.A., Burt, R.M., Cole, J.W., Krippner, S.J.P., Price, R.C., Cartwright, I., 1998. Plutonic lithics in ignimbrites of Taupo Volcanic Zone, New Zealand: sources and conditions of crystallisation. Chemical Geology 148, 21–41.
Browne, P.R.L., Graham, I.J., Parker, R.J., Wood, C.P., 1992. Subsurface andesite lavas and plutonic rocks in the Rotokawa and Ngatamariki geothermal systems, Taupo Volcanic Zone, New Zealand. Journal of Volcanology and Geothermal Research 51, 199–215.
Bryan, C.J., Sherburn, S., Bibby, H.M., Bannister, S.C., Hurst, A.W., 1999. Shallow seismicity of the central Taupo Volcanic Zone, New Zealand: its distribution and nature. New Zealand Journal of Geology and Geophysics 42, 533–542.
Burt, R.M., Brown, S.J.A., Cole, J.W., Shelley, D., Waight, T., 1998. Glass-bearing plutonic fragments from ignimbrites of the Okataina caldera complex, Taupo Volcanic Zone, New Zealand; remnants of a partially molten intrusion associated with preceding eruptions. Journal of Volcanology and Geothermal Research 84, 209–237.
Charlier, B.L.A., Wilson, C.J.N., 2010. Chronology and evolution of caldera-forming and post-caldera magma systems at Okataina Volcano, New Zealand from zircon U–Th model-age spectra. Journal of Petrology 51, 1121–1141.
Charlier, B.L.A., Peate, D.W., Wilson, C.J.N., Lowenstern, J.B., Storey, M., Brown, S.J.A., 2003. Crystallisation ages in coeval silicic magma bodies; ^{238}U–^{230}Th disequilibrium evidence from the Rotoiti and Earthquake Flat eruption deposits, Taupo volcanic zone, New Zealand. Earth and Planetary Science Letters 206, 441–457.
Charlier, B.L.A., Wilson, C.J.N., Lowenstern, J.B., Blake, S., van Calsteren, P.W., Davidson, J.P., 2005. Magma generation at a large, hyperactive silicic volcano (Taupo, New Zealand) revealed by U–Th and U–Pb systematics in zircons. Journal of Petrology 46, 3–32.
Cole, J.W., Spinks, K.D., Deering, C.D., Nairn, I.A., Leonard, G.S., 2010. Volcanic and structural evolution of the Okataina Volcanic Centre; dominantly silicic volcanism associated with the Taupo Rift, New Zealand. Journal of Volcanology and Geothermal Research 190, 123–135.
Ewart, A., Cole, J.W., 1967. Textural and mineralogical significance of granitic xenoliths from the central volcanic region, North Island, New Zealand. New Zealand Journal of Geology and Geophysics 10, 31–54.
Ewart, A., Griffin, W.L., 1994. Application of proton microprobe data to trace element partitioning in volcanic rocks. Chemical Geology 117, 251–284.
Harvey, P.K., Taylor, D.M., Hendry, R.D., Bancroft, F., 1973. X-ray spectrometry. An Accurate Fusion Method for the Analyses of Rocks and Chemically Related Materials by X-Ray Fluorescence Spectrometry. Heyden and Son, London, pp. 33–44.
Heise, W., Caldwell, T.G., Bibby, H.M., Bennie, S.L., 2010. Three-dimensional electrical resistivity image of magma beneath an active continental rift, Taupo Volcanic Zone, New Zealand. Geophysical Research Letters 37. doi:10.1029/2010GL043110.
Hildreth, W., 2004. Volcanological perspectives on Long Valley, Mammoth Mountain, and Mono Craters; several contiguous but discrete systems. Journal of Volcanology and Geothermal Research 136, 169–198.
Jurado-Chichay, Z., Walker, G.P.L., 2000. Stratigraphy and dispersal of the Mangaone Subgroup pyroclastic deposits, Okataina Volcanic Centre, New Zealand. Journal of Volcanology and Geothermal Research 104, 319–380.
Kerrich, R., Wyman, D.A., 1996. The trace element systematic of igneous rocks in mineral exploration: an overview. Geological Association of Canada, Short Course Notes 12, 1–50.
Klemetti, E.W., Deering, C.D., Cooper, K.M., Roeske, S.M., 2011. Magmatic perturbations in the Okataina Volcanic Complex, New Zealand at thousand-year timescales recorded in single zircon crystals. Earth and Planetary Science Letters 305, 185–194.
Lowe, D.J., Shane, P.A.R., Alloway, B.V., Newnham, R.W., 2008. Fingerprints and age models for widespread New Zealand tephra marker beds erupted since 30,000 yr ago as a framework for NZ-INTIMATE. Quaternary Science Reviews 27, 95–126.
Lowenstern, J.B., Clynne, M.A., Bullen, T.B., 1997. Comagmatic A-type granophyre and rhyolite from the Alid Volcanic Center, Eritrea, Northeast Africa. Journal of Petrology 38, 1707–1721.
Lowenstern, J.B., Persing, H.M., Wooden, J.L., Lanphere, M.A., Donnelly-Nolan, J.M., Grove, T.L., 2000. U–Th dating of single zircons from young granitoid xenoliths: new tools for understanding volcanic processes. Earth and Planetary Science Letters 183, 291–302.
Ludwig, K.R., 2003. Isoplot/Ex version 3.41, A Geochronological Toolkit for Microsoft Excel. Berkeley Geochronology Center Special Publication, 4.
Mahon, K., 1996. The New 'York' regression: application of an improved statistical method to geochemistry. International Geological Review 38, 293–303.
Mahood, G., Hildreth, W., 1983. Large partition coefficients for trace elements in high-silica rhyolite. Geochimica et Cosmochimica Acta 47, 11–30.
McCormack, K.D., Gee, M.A.M., McNaughton, N.J., Smith, R., Fletcher, I.R., 2009. U–Pb dating of magmatic and xenocryst zircons from Mangakino ignimbrites and their correlation with detrital zircons from the Torlesse metasediments, Taupo Volcanic Zone, New Zealand. Journal of Volcanology and Geothermal Research 183, 97–111.
Nairn, I.A., 2002. Geology of the Okataina Volcanic Centre. Institute of Geological & Nuclear Sciences Geological Map 25, 25. Institute of Geological & Nuclear Sciences, Lower Hutt, New Zealand, 156 + 1 sheet pp.
Nairn, I.A., Self, S., Cole, J.W., Leonard, G.S., Scutter, C., 2001. Distribution, stratigraphy, and history of proximal deposits from the c. AD 1305 Kaharoa eruptive episode at Tarawera Volcano, New Zealand. New Zealand Journal of Geology and Geophysics 44, 467–484.
Nairn, I.A., Shane, P.R., Cole, J.W., Leonard, G.J., Self, S., Pearson, N., 2004. Rhyolite magma processes of the approximately AD 1315 Kaharoa eruption episode, Tarawera Volcano, New Zealand. Journal of Volcanology and Geothermal Research 131, 265–294.
Paces, J.B., Miller, J.D., 1993. Precise U–Pb ages of Duluth Complex and related mafic intrusions, northeastern Minnesota; geochronological insights to physical, petrogenetic, paleomagnetic, and tectonomagnetic processes associated with the 1.1 Ga Midcontinent Rift System. Journal of Geophysical Research 98, 13997–14013.
Schmitt, A.K., 2011. Uranium series accessory crystal dating of magmatic processes. Annual Review of Earth and Planetary Sciences 39, 321–349.
Schmitt, A.K., Hulen, J.B., 2008. Buried rhyolites within the active, high-temperature Salton Sea geothermal system. Journal of Volcanology and Geothermal Research 178, 708–718.
Schmitt, A.K., Vazquez, J., 2006. Alteration and remelting of nascent oceanic crust during continental rupture: evidence from zircon geochemistry of rhyolites and xenoliths from the Salton Trough, California. Earth and Planetary Science Letters 252, 260–274.
Schmitt, A.K., Grove, M., Harrison, T.M., Lovera, O., Hulen, J., Walters, M., 2003. The Geysers–Cobb Mountain Magma System, California (Part 1): U–Pb zircon ages of volcanic rocks, conditions of zircon crystallization and magma residence times. Geochimica et Cosmochimica Acta 67, 3423–3442.
Schmitt, A.K., Stockli, D.F., Hausback, B.P., 2006. Eruption and magma crystallization ages of Las Tres Vírgenes (Baja California) constrained by combined $^{230}Th/^{238}U$ and (U–Th)/He dating of zircon. Journal of Volcanology and Geothermal Research 158, 281–295.
Schmitt, A.K., Stockli, D.F., Lindsay, J.M., Robertson, R., Lovera, O.M., Kislitsyn, R., 2010. Episodic growth and homogenization of plutonic roots in arc volcanoes from combined U–Th and (U–Th)/He zircon dating. Earth and Planetary Science Letters 295, 91–103.
Seebeck, H., Nicol, A., Stern, T.A., Bibby, H.M., Stagpoole, V., 2010. Fault controls on the geometry and location of the Okataina Caldera, Taupo Volcanic Zone, New Zealand. Journal of Volcanology and Geothermal Research 190, 136–151.
Shane, P., Sandiford, A., 2003. Paleovegetation of Marine Isotope Stage 4 and 3 in Northern New Zealand and the age of the widespread Rotoehu tephra. Quaternary Research 59, 420–429.
Shane, P., Smith, V.C., Nairn, I., 2008a. Millennial timescale resolution of rhyolite magma recharge at Tarawera Volcano; insights from quartz chemistry and melt inclusions. Contributions to Mineralogy and Petrology 156, 397–411.
Shane, P., Nairn, I.A., Smith, V.C., Darragh, M., Beggs, K., Cole, J.W., 2008b. Silicic recharge of multiple rhyolite magmas by basaltic intrusion during the 22.6 ka Okareka Eruption Episode, New Zealand. Lithos 103, 527–549.
Storm, S., Shane, P., Schmitt, A.K., Lindsay, J.M., 2011. Contrasting punctuated zircon growth in two syn-erupted rhyolite magmas from Tarawera Volcano: insights to

crystal diversity in magmatic systems. Earth and Planetary Science Letters 301, 511–520.
Storm, S., Shane, P., Schmitt, A.K., Lindsay, J.M., in press. Decoupled crystallization and eruption histories of the rhyolite magmatic system at Tarawera volcano revealed by zircon ages and growth rates. Contributions to Mineralogy and Petrology. doi:10.1007/s00410-011-0682-8.
Sun, S., McDonough, W.F., 1989. Chemical and isotopic systematic of oceanic basalts: implications for mantle composition and process. In: Saunders, A.D., Norry, M.J. (Eds.), Magmatism in the Ocean Basins: Geological Society of London, Special Publication, Vol. 42, pp. 313–345.
Trail, D., Mojzsis, S.J., Harrison, T.M., Schmitt, A.K., Watson, E.B., Young, E.D., 2007. Constraints on Hadean zircon protoliths from oxygen isotopes, REEs and Ti-thermometry. Geochemistry, Geophysics, Geosystems 8 (6). doi:10.1029/2006GC001449.
Trail, D., Bindeman, I.N., Watson, E.B., Schmitt, A.K., 2009. Experimental calibration of oxygen isotope fractionation between quartz and zircon. Geochimica et Cosmochimica Acta 73, 7110–7126.
Vazquez, J.A., Shamberger, P.J., Hammer, J.E., 2007. Plutonic xenoliths reveal the timing of magma evolution at Hualalai and Mauna Kea, Hawaii. Geology 35, 695–698.
Watson, E.B., Harrison, T.M., 1983. Zircon saturation revisited: temperature and composition effects in a variety of crustal magma types. Earth and Planetary Science Letters 64, 295–304.
White, S.M., Crisp, J.A., Spera, F.J., 2006. Long-term volumetric eruption rates and magma budgets. Geochemistry, Geophysics, Geosystems 7, Q03010. doi:10.1029/2005GC001002.
Wilson, C.J.N., Charlier, B.L.A., 2009. Rapid rates of magma generation at contemporaneous magma systems, Taupo Volcano, New Zealand; insights from U–Th model-age spectra in zircons. Journal of Petrology 50, 875–907.
Wiedenbeck, M., Alle, P., Corfu, F., Griffin, W.L., Meier, M., Oberli, F., Von Quadt, A., Roddick, J.C., Spiegel, W., 1995. Three natural zircon standards for U-Th-Pb, Lu-Hf, trace element and REE analyses. Geostandards Newsletter 19, 1–23.
Wilson, C.J.N., Rhoades, D.A., Lanphere, M.A., Calvert, A.T., Houghton, B.F., Weaver, S.D., Cole, J.W., 2007. A multiple-approach radiometric age estimate for the Rotoiti and Earthquake Flat eruptions, New Zealand, with implications for the MIS 4/3 boundary. Quaternary Science Reviews 26, 1861–1870.
Wilson, C.J.N., Charlier, B.L.A., Fagan, C.J., Spinks, K.D., Gravley, D.M., Simmons, S.F., Browne, P.R.L., 2008. U–Pb dating of zircon in hydrothermally altered rocks as a correlation tool: application to the Mangakino geothermal field, New Zealand. Journal of Volcanology and Geothermal Research 176, 191–198.
Wilson, C.J.N., Gravley, D.M., Leonard, G.S., Rowland, J.V., 2009. Volcanism in the central Taupo Volcanic Zone, New Zealand: tempo styles and controls. In: Thordarson, T., et al. (Ed.), Studies in Volcanology: The Legacy of George Walker: IAVCEI Proceedings in Volcanology, 2.